An Empirical Model for a CO_2 Thermal Compressor Based on Experimental Data

Ali Salame[1,2,3], Vincent Lemort[2], Pascal Dufour[3], Madiha Nadri[3], Rabah Ibsaine[1],

[1]Boostheat Company,
Lyon, France,
(+33) 0 6 70 84 61, ali.salame@boostheat.com

[2]University of Liège, Energy Systems Research Unit,
Liège, Belgium,
vincent.lemort@uliege.be

[3] Univ Lyon, Université Claude Bernard Lyon 1, CNRS, LAGEPP UMR 5007,
43 boulevard du 11 novembre 1918, F-69100, VILLEURBANNE, France,
pascal.dufour@univ-lyon1.fr

ABSTRACT

A thermal compressor uses thermal energy to increase the pressure of the working gas, while maintaining a temperature difference, as an essential factor for its effective functioning. BoostHEAT's innovative thermal compressor, driven by eco-friendly thermal energy, not only targets the replacement of traditional compressors in various CO_2 applications, but also aligns with the critical environmental motive to address global warming. The design of the targeted thermal compressor is inspired by the gamma type Stirling engine, replacing the power piston with inlet and outlet valves**.** In this paper, the thermal compressor (treated as a black box) is implemented in a heat pump cycle, on which the tests were conducted**.** In the context of thermodynamic analysis, six principal inputs are imposed to the compressor, and five outputs are measured. These physical variables are crucial in characterizing the compressor, and evaluating its perfromance. An empirical model is developed where each output is represented as a function of these inputs in a general mathematical form. The objective is to fine-tune these functions using machine learning regression methods, based on the collected data. A sensitivity analysis is carried on each output with respect to the inputs, in order to investigate the correlations between them and find the relevant inputs for each selected output.

1. INTRODUCTION

Heating systems are major contributors to the overall energy consumption and greenhouse gases. So, reducing these two factors would necessarily need more environmentally friendly heating systems. Among them are the heat-driven heat pump cycles, where heating methods are combined with heat pump cycles. Some examples include non-integrated systems that involve the coupling of a Stirling engine with a traditional electric compressor, and integrated ones such as the Vuilleumier machines introduced by Bush (1939) patent, that operates on the principles of a Stirling engine, absorbing heat to produce cooling and heating through compression and expansion processes. An application is a Stirling type thermal compressor introduced by Ibsaine et al. (2016), which is a thermally driven compressor that aim to replace a traditional compressor in a heat pump cycle. Another environmental advantage of this technology was the use of CO_2 as the refrigerant, which have a relatively low global warming potential and 0 ozone depletion, along with its non-toxic and non-flammable characteristics.
A thermal compressor is a gamma type Stirling engine having the power piston replaced with inlet and outlet valves. Therefore, the main components are two working spaces (compression (C) and expansion (E)) that are connected with heat exchangers, heater (H), cooler (K) and regenerator (R). The heat is received through the heater and rejected through the cooler. Both heat exchangers are separated with a porous medium regenerator that acts as a thermal capacitor to ensure a temperature difference between lower and upper parts. A displacer separating the two

working spaces is coupled to an electric motor with a crank mechanism and used to transport the fluid inside the thermal compressor between lower cold and top hot parts. In few words, a thermal compression process can be divided into 4 phases that are illustrated in Figure 1 showing the variation of the CO_2 pressure as a function of the displacer displacement. From phase 1 to 2, the displacer descent pushes the CO_2 to the cylinder upper hot section. As a result of the elevated temperatures, the fluid pressure starts to rise incrementally. Upon reaching sufficient pressure, the exhaust valve activates, and CO_2 is held at a steady pressure from phases 2 to 3, with no pressure loss from valve flow assumed. At phase 3, the displacer shifts its movement direction, moving the CO_2 back to the cooler lower section, which leads to a steady pressure decline. As the pressure drops to a sufficient level by phase 4, the inlet valve opens, allowing the CO_2 to revert to its original state at phase 1.

Most of the attempts to model a thermal compressor were based on physical equations. To the authors' best knowledge, no statistical based model was derived for a Stirling type thermal compressor. Although such model would lack important physical aspects inside, it provides a fast and reliable performance predictions based on real experimental data. The collected data is from 3 separate setups of almost similar test bench layout, which is introduced in the second section. The third section introduces the machine learning (ML) models that are to be used to predict the compressor performance. In section four, a sensitivity analysis is introduced to sort the order of effectiveness of the independent variables on each dependent variable, to find the relevant inputs for each. The data is then fitted into 3 types of ML models, where a comparison of their accuracy is shown in parity plots with the Mean Absolute Prediction Error (MAPE) and the R^2 of each.

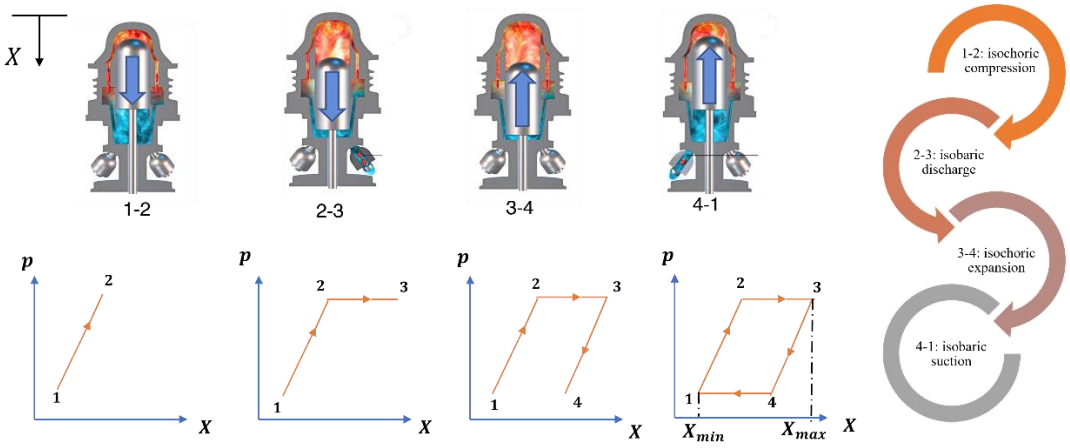

Figure 1: Thermal compression process described by the variation of pressure inside as a function of the position *X* of the displacer.

2. Experimental Setup

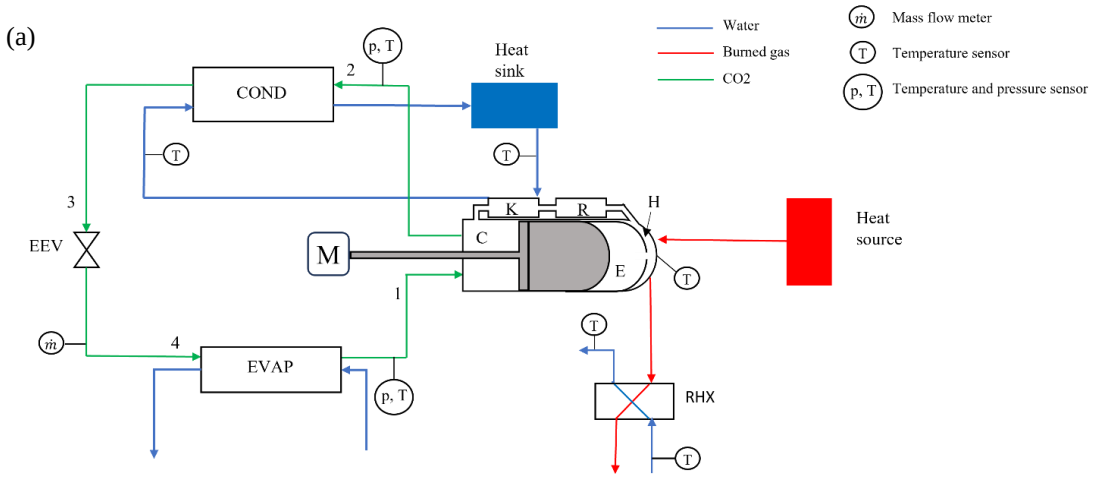

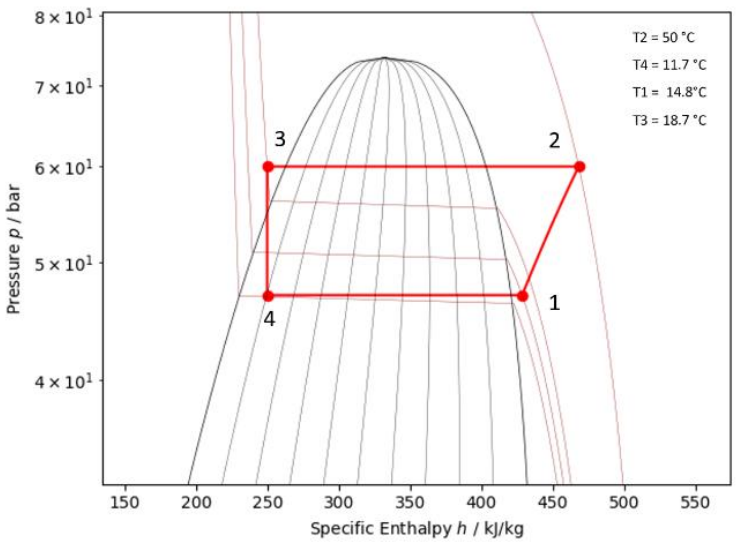

Figure 2: (a) Test Bench layout with (b) the pH diagram of CO_2 in the cycle.

The thermal compressor was installed in a basic heat pump cycle shown in figure 2 (a). It consists of a compressor (CP), a condenser (COND), an electronic expansion valve (EEV), and an evaporator (EVAP). The EEV is manually adjusted to regulate the inlet and outlet pressures p_{in} and p_{out}. The CO_2 in the cycle remains in its subcritical state, as seen in the p-h diagram figure 2 (b).

The thermal compressor is accompanied with a heat combustion process on the top, where part of the heat is absorbed ($P_{heating}$), and the rest is recovered by a recovery heat exchanger (RHX) in the form of waste heat. An electric motor (M) with power (P_{motor}) is connected to the displacer to ensure its movement, but with a relatively low power compared to the combustion power. Part of the resulting power is recovered by the cooling water ($P_{cooling}$) that circulates around K in a water jacket, and the rest is released to the thermal cycle as an output enthalpy flow (T_{out} and $\dot{m}$). The overall ranges of the independent variables (inputs) in the three different experiments are:

- p_{in}: inlet pressure ∈ [23, 48.7] bar.
- p_{out}: outlet pressure ∈ [34.4, 64.2] bar.
- ω: motor rotation speed ∈ [60, 260] rpm.
- T_{heater}: heater temperature ∈ [300, 800] °C.
- T_w: cooling water temperature ∈ [17.5, 41.8] °C.
- T_{in}: evaporation temperature or temperature of CO_2 entering the compressor ∈ [1.6, 26.8] °C.

While the resulting outputs (dependent variables) ranges are:

- $\dot{m}$: mass flow rate of CO2 ∈ [3.6, 46] g/s.
- $P_{heating}$: Heating power absorbed by the compressor ∈ $[461, 3774]W$.
- $P_{cooling}$: Cooling power or heat rejected to the cooling water ∈ $[441, 2581]W$.
- P_{motor}: Electric power provided to the motor ∈ $[-38, 302]W$.
- T_{out}: Outlet temperature ∈ $[37, 83]°C$.

2.1 Performance curves

Based on the collected data, we show the performance of the tested thermal compressor. Mass flow rate and heating power, being the two main performance indicators of a thermal compressor are plotted as a function of pressure ratio $P_r = \frac{p_{out}}{p_{in}}$, temperature ratio $T_r = \frac{T_{heater}\,[K]}{T_w\,[K]}$, and motor speed ω:

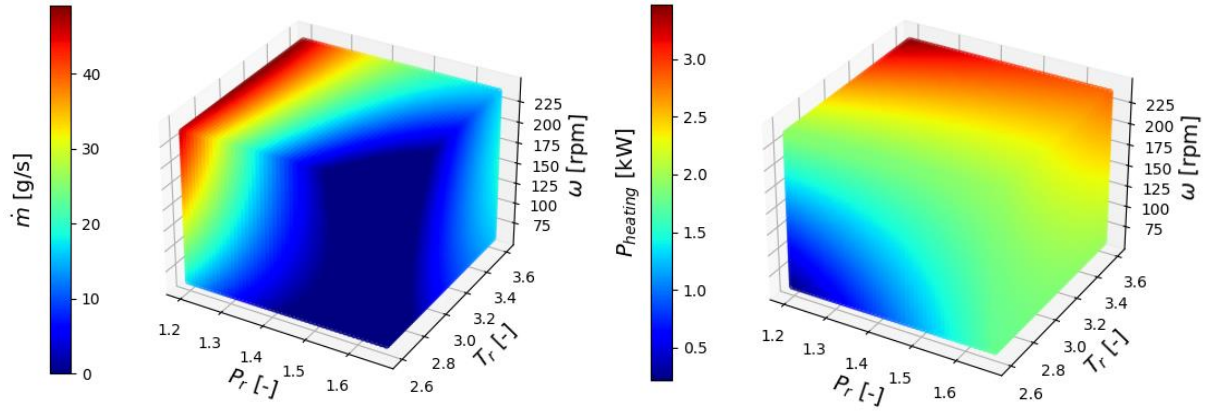

Figure 3: 3D plots showing the variation of $\dot{m}$ and $P_{heating}$ as a function of $P_r, T_r, and\ \omega$.

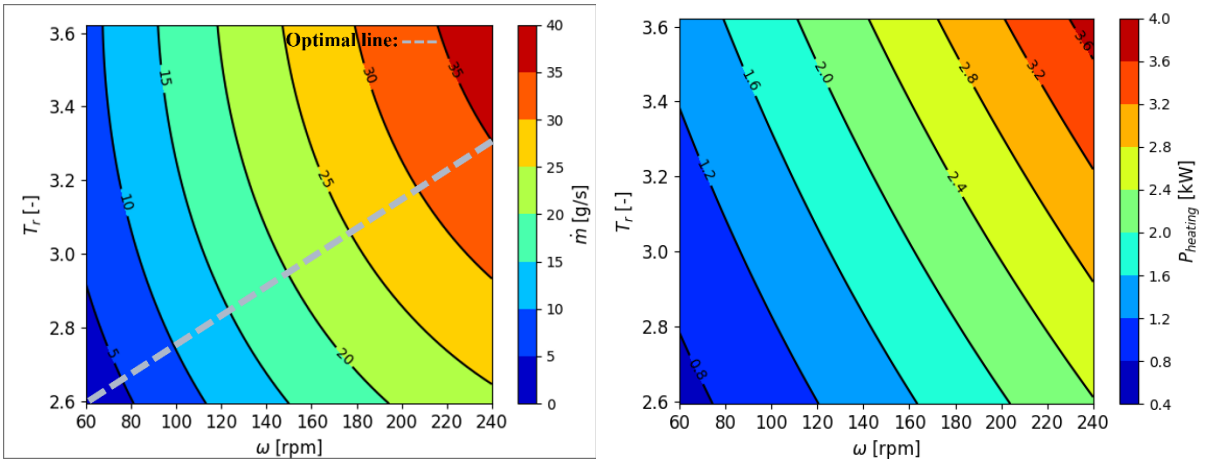

Figure 4: 2D plots showing the variation of (a) $\dot{m}$ and (b) $P_{heating}$ as a function of $T_r\ and\ \omega$, at $P_r = 1.3$.

Figure 4 (b) shows a linear variation of the heating power curves, while such curves are of parabolic shapes for what concerns the mass flow rate. Therefore, the same mass flow rates can be obtained at various heating power values. An optimal line is drawn on figure 4 (a) depicting the optimal (ω, T_r) values that provide highest mass flow rate values at minimum heat power values for $P_r = 1.3$.

3. ML models

3.1 Regression Models

Regression models are fundamental tools in statistics and machine learning for understanding the relationship between a dependent variable and one or more independent variables as developed in James al. (2013) book. The goal of regression analysis is to model the expected value of the dependent variable based on the values of the independent variables. Yazar et al. (2017) have compared various regression models that were developed to predict the parameters of a compressor and a turbine. Among these models, a linear Regression (LR) is the simplest form of regression that assumes a linear relationship between the dependent variable and independent variables. Let $y_p = [y_1, y_2, \dots, y_n]$ be the predicted output vector, with n as the number of observations. Each predicted output of a single observation can be described in the form:

$$y_k = \beta_0 + \sum_{i=1}^{l} \beta_i x_{ki}$$

Where y_k is the predicted value for the k-th observation, x_{ki} are the input features, β_0 is the intercept of the model, β_i are the coefficients of the inputs x_{ki}, and l is the number of inputs which in our case is equal to six. The optimal model coefficient (β) is determined by solving the ordinary least squares (OLS) minimization problem, which aims to minimize the squared differences between the predicted values y_p and the actual data values y_r. The OLS objective function can be expressed as:

$$\min_{\beta} \sum (y_p - y_r)^2$$

The LR and polynomial regression (PR) models are derived using 'Sklearn' or scikit-learn library in python, which comes with several built-in ML algorithms. 80 % of the data is used to train the model, while the rest is used for validating it.

3.2 ANN Model

Artificial Neural Networks (ANNs) are a cornerstone of machine learning, inspired by the structure and functional aspects of biological neural networks as described in the book of Haykin (2009). An ANN is composed of interconnected processing elements, known as neurons which are organized into layers (input, hidden, and output) to process data. Each neuron performs a linear regression—applying weights w_i, summing inputs x_i, and potentially using an activation function f to introduce non-linearity—before passing the result to subsequent neurons. b_k is a bias parameter that helps adjust the output of a neuron independently of its inputs. An output of a $k-th$ neuron is expressed as follows:

$$y_k = f\left(\sum_{i=1}^{l} w_{ki} x_{ki} + b_k\right)$$

In the context of regression, the model aims to predict continuous outcomes by adjusting the weights between neurons to minimize prediction error, through a process of training and optimization. This structured approach allows neural networks to capture complex patterns within the data, facilitating accurate predictions on new, unseen datasets, and making them particularly suitable for sophisticated regression tasks in a wide array of research and application fields.

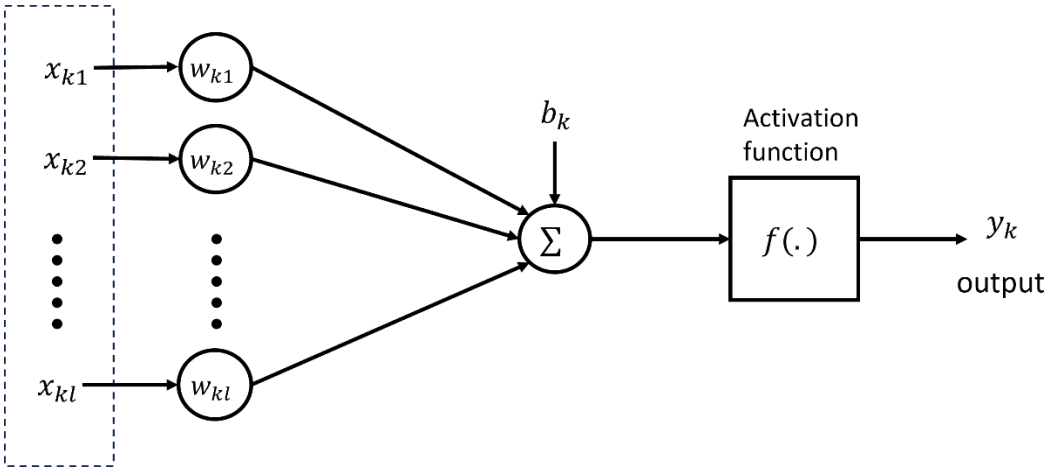

Figure 5: Structure of k-th neuron of ANN model.

Ziviani et al. (2018) have developed an ANN model for a scroll expander and an injected scroll compressor type, achieving a higher accuracy than a semi-empirical model, as an ANN model needs no assumptions and can be

directly trained with experimental data. In this sense, we develop an ANN model for the tested thermal compressor. The model of each output variable consists of an input and a hidden layer of a maximum of 300 neurons and an output layer of 1 neuron. Rectifier linear unit (ReLU) is applied on all the layers, 'Adamax' is chosen as the learning algorithm, and 'Mean squared error' as the error function with 0.2 as validation set. To increase the nonlinearity and the accuracy of the ANN model, more hidden layers and neurons can be added, but at a higher risk of overfitting. The derivation of the ANN model was done using Keras introduced by Chollet (2015), which is a high-level neural network application program interface, written in python and directly integrated in TensorFlow.
A common indicator of the fit quality of a regression model is the R^2 metric, which quantifies how close is the data to the regression model predictions by the following ratio:

$$R^2 = 100\% \frac{cov(y_r, y_p)}{\sqrt{cov(y_r, y_r).cov(y_p, y_p)}}$$

A close value to 100% R^2 indicates a perfect fit, which would indicate that the model is overfitted. To make sure the predictions are not biased, a second indicator is introduced referred to as the mean absolute percentage error (MAPE). Which can be represented by the following equation:

$$MAPE = \frac{100\%}{n} \sum \left| \frac{y_p - y_r}{y_r} \right|$$

A 0 % MAPE indicates a perfect fit. Before comparing the models' accuracies, a sensitivity analysis is carried out to evaluate the impact of the input variables on each respective output variable. To guarantee a scale uniformity of the inputs, the training and the testing data are normalized between (0.1, 0.9) by applying:

$$x_{norm} = 0.8 \frac{x - x_{min}}{x_{max} - x_{min}} + 0.1$$

Where x_{min} and x_{max} are the minimum and maximum values of the defined vector x, and x_{norm} is the resulting normalized vector.

4. Results and Discussions

4.1 Sensitivity Analysis

In this section, we analyze the sensitivity of each output with respect to the 6 inputs defined previously. The data is first fitted into a Gaussian process model, and the automatic relevance determination (ARD) is chosen as its Kernel. As indicated by Quoilin and Schrouff (2016), this Kernel allows the determination of the length scale of the inputs, where the highest value represents the least relevant input for the selected output. To increase the effectiveness of this method, a cross validation of 10 folds is applied on each Gaussian model, and the length scale for each is then determined as the average of all cross-validations. The resulting length scale of each output are as follows:

Table 1: length scale values of the inputs corresponding to each output.

	p_{in}	p_{out}	ω	T_{heater}	T_w	T_{in}
$\dot{m}$	0.5	0.37	0.62	0.6	0.48	20.35
$P_{heating}$	0.51	0.65	0.93	0.18	0.77	0.98
$P_{cooling}$	0.55	0.2	0.3	0.83	1.2	0.6
P_{motor}	0.44	0.33	0.35	0.27	1.14	4.9
T_{out}	0.35	0.55	1.13	0.35	1.15	0.7

Higher length scale values are seen in T_w and T_{in}. To further verify the inputs impacts on the outputs, each of the outputs is obtained with different sets of inputs by fitting them in PR models and comparing the MAPE and R^2 values for each. As seen in the figures below, the highest variation of MAPE and R^2 on all outputs except T_{out} is

caused by the addition of ω as one of the inputs, which shows that ω has the strongest impact. On the other hand, T_{in} seems to have the least impact on all the outputs. It's interesting to see that P_{motor} can reach a satisfying prediction (> 93 % R^2 and < 8 % MAPE) with $p_{in}, p_{out}, and\ \omega$ as the inputs, while $P_{cooling}$ and $P_{heating}$ would need T_{heater} as a fourth input to achieve such accuracy. For $\dot{m}$ and T_{out} at least first five inputs are needed. As a result, T_{in} is disregarded in the next section, and the derived models will be dependent on the five first inputs, $p_{in}, p_{out}, \omega, T_{heater}$, and T_w.

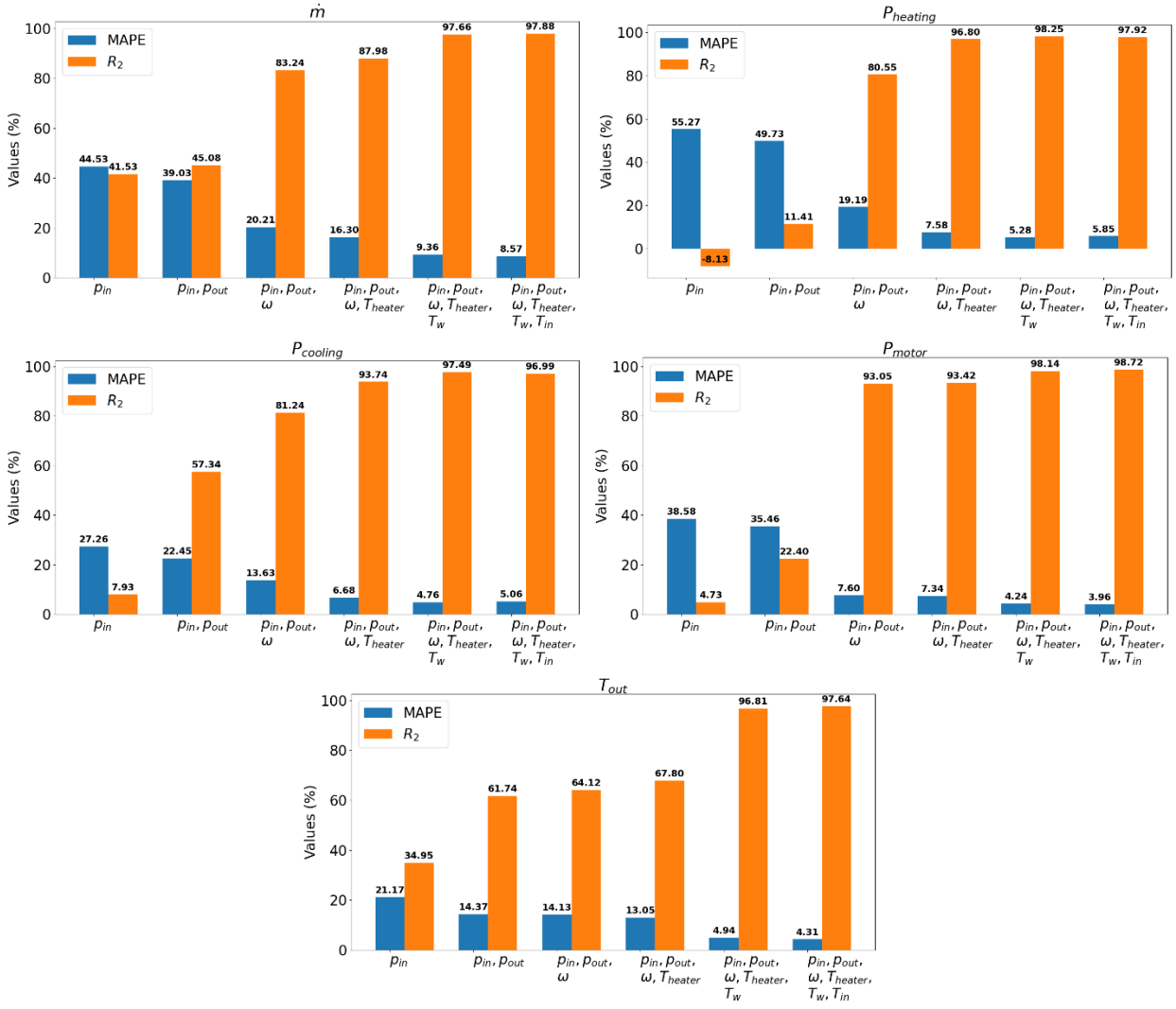

Figure 6: MAPE and R^2 values of PR models with different sets of inputs.

4.2 Models Accuracies

From 3 different test benches, 251 samples are collected, and used to derive the data-based models. The shown plots correspond to 20 % of the 251 points that are used to compare the accuracies of the models. As a result, the ANN model showed the highest predictions accuracy, with not much difference from the PR predictions. Even the LR predictions are not very distant from the 2 other nonlinear models for $P_{heating}, P_{cooling}$, and T_{out} outputs. An advantage of having a good accuracy for PR models is the ability to represent them in algebraically.

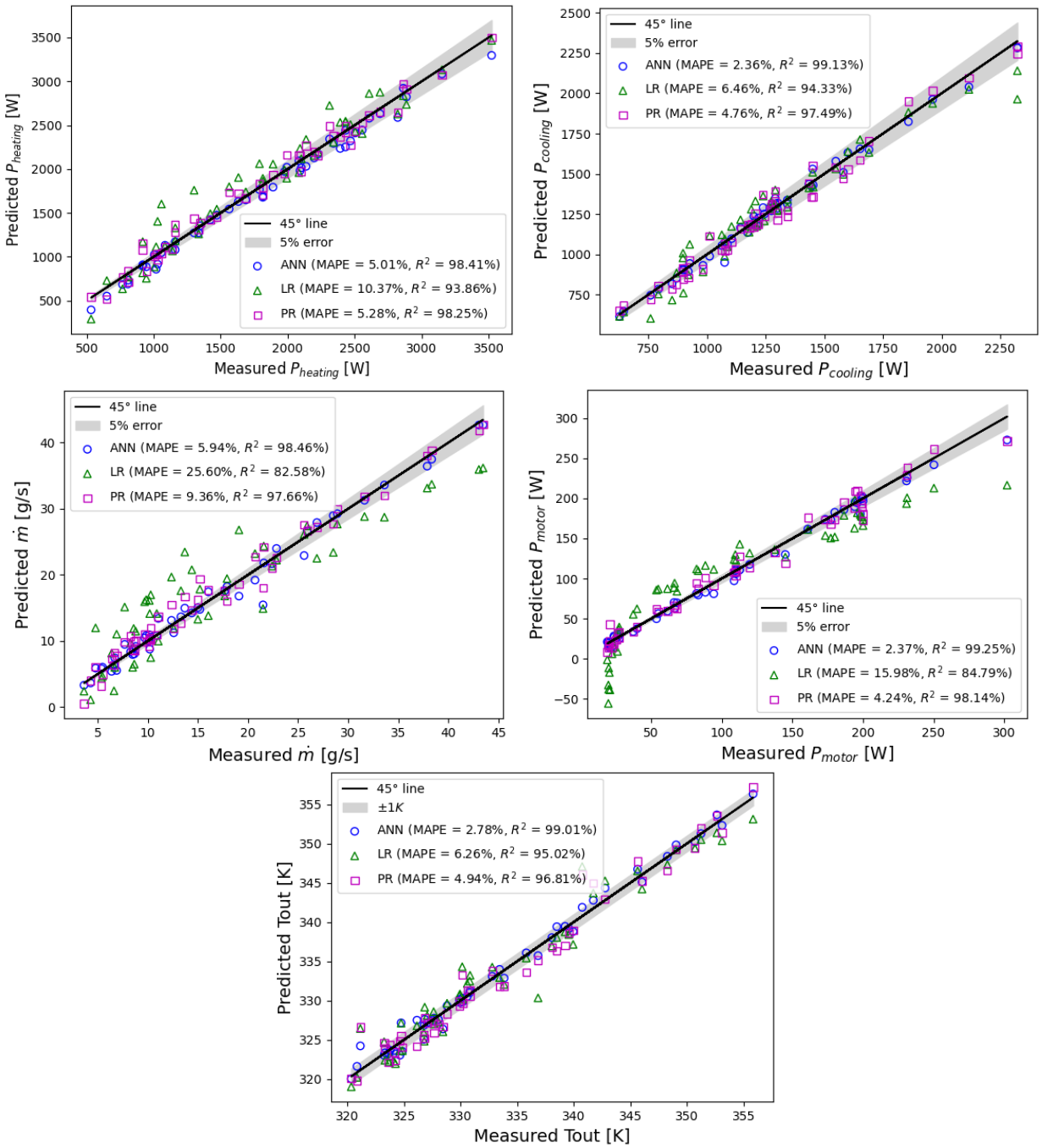

Figure 7: Accuracies of LR, PR, and ANN models.

5. Conclusion

A Stirling type CO_2 thermal compressor for heat pump applications was introduced. The compressor was tested in a heat pump test bench cycle. The collected data included six main inputs and five outputs that are used to plot the performance curves of the thermal compressor. A sensitivity analysis is applied to determine the relevant inputs and sort the impact of each of the inputs on each output. An artificial neural network (ANN), linear regression (LR) and polynomial regression (PR) models are obtained taking the relevant inputs for each output as the independent variables. The three methods are then compared, showing a highest accuracy for the ANN model, closely followed

by the PR model. Obtaining it can reliably be used in ML tools are reliable to analyze the data, the correlations between them, and empirical models to predict the performance, both reliably and fast.

NOMENCLATURE

X	displacement of displacer	(m)
b_k	k-th bias	(-)
y_p	predicted output vector	(-)
y_k	single predicted output	(-)
y_r	real value	(-)
x	inputs vector	(-)
l	number of inputs	(-)
n	number of observations	(-)
p_{in}	inlet pressure	(Pa)
p_{out}	outlet pressure	(Pa)
T_{heater}	Heater temperature	(K)
T_w	Water temperature	(K)
ω	motor speed	(Rpm)
$\dot{m}$	mass flow rate	(g/s)
$P_{heating}$	heating power	(W)
$P_{cooling}$	cooling power	(W)
P_{motor}	motor power	(W)
T_{out}	outlet temperature	(K)

Subscripts

CO_2	Carbon dioxide
ML	machine learning
max	maximum
min	minimum
H	heater
R	regenerator
K	cooler
C	compression
E	expansion

REFERENCES

Bush, V., (1939). "Apparatus for compressing gases," *US Patent 2,157,229*.

Chollet, F., (2015). Keras. Github. Retrieved from https://github.com/fchollet/keras.

Haykin, S., (2009). Neural Networks and Learning Machines (3rd Edition ed.). Pearson Practice Hall.

Ibsaine, R., Joffroy, J.M., Stouffs, P., (2016). Modelling of a new thermal compressor for supercritical CO_2 heat pump, *Energy*, Volume 117, Part 2, p. 530-539.

James, G., Witten, D., Hastie, T., Tibshirani, R., (2013). An Introduction to Statistical Learning with Applications in R, New York: Springer.

Quoilin S., Schrouff J., Assessing Steady-State, Multivariate Experimental Data Using Gaussian Processes: The GPExp Open-Source Library. *Energies*. 2016; 9(6):423.

Yazar, I., Yavuz, H.S., Yavuz, A.A., (2017). Comparison of various regression models for predicting compressor and turbine performance parameters, *Energy*, Volume 140, Part 2, Pages 1398-1406.

Ziviani, D., Ammar M.B., Nelson A.J., Dominique L., James E.B. and Eckhard A.G., (2018). Machine Learning Applied to Positive Displacement Compressors and Expanders Performance Mapping.